IMPROVED LOUDSPEAKER ARRAY MODELING

PART 2

David W. Gunness and William R. Hoy

Eastern Acoustic Works, Inc.
1 Main St., Whitinsville, MA 01588
PH: 508-234-6158 FAX: 508-234-6479
e-mail: david.gunness@eaw.com, bhoy@eaw.com

ABSTRACT

The modeling technique presented in Part 1 is extended to three-dimensional space through the use of a flat tessellation of the horn mouth. This is made possible by a more complete version of the Kirchoff-Helmholtz integral, which is applicable to a surface of arbitrary shape. The three-dimensional technique is effective with asymmetrical devices, and produces better agreement with measurements at low frequencies and at angles near and beyond 90° off axis.

0 INTRODUCTION

0.1 Tessellation Method Presented in Part 1

In "Improved Loudspeaker Array Modeling" (Part 1), presented at the AES 107th Convention in New York, a new method of modeling horn directionality was presented, which incorporated the known size and shape of the horn [1]. By constructing the wavefront emanating from a horn as a mosaic of tiles, called *tessellae*, the directional response of a horn could be accurately represented. One tessella replaced many point sources, so the model was very efficient, computationally.

The examples in that paper employed rectangular tessellae, characterized by their length, width, rotation, elevation, and azimuth. Working in a three-dimensional CAD program, a presumed wavefront was constructed by developing a curve that was equidistant from the original source of sound (Huygen's Construction [2][3]). In the case of horn modeling, the shortest path from the horn throat was used to define the surface. A second requirement was that all output from the source had to pass through the defining surface, and propagate unimpeded thereafter. This requirement can only be met if the edges of the tessellation model coincide with the edges of the mouth.

The surface, as defined, was tiled with a number of rectangular tessellae, and their physical descriptions were transferred via data exchange format (.dxf) file to a specialized modeling program. The software model was constructed to precisely match the measurement setup that was used to obtain the directional response of the subject horn. The directional response of the software model, represented by a family of complex frequency-response curves, agreed surprisingly well with the measured data.

In order to improve the agreement further, a “driving function” for each tessella was adjusted. The driving functions included gain, delay, and low-pass filtering, which allowed the wavefront shape to be fine-tuned, and allowed the model to account for throat beaming and high frequency shadowing due to bends in the horn walls. A programmed optimizer adjusted the driving function parameters, to achieve the best possible match between modeled and measured data. After modeling a single horn, the same technique was applied to arrays of horns, with equally good agreement between modeled and measured results.

Tessellation proved to be a promising technique. The method was free from apparent apex errors, and there was no distance variation or focal error if the source was not positioned at the center of rotation. Tessellation also proved to be fully inclusive – interpolated results matched just as closely as the “training curves”. Once a model was built and “trained,” full resolution data could be obtained at any angle in the valid range.

Unfortunately, the tessellation technique had some limitations. Because the model for an individual tessella is front-to-back symmetrical, the accuracy deteriorates as the point of observation is moved beyond 90° off the axis of one or more tessellae. Furthermore, the angular region of validity was smaller for arced arrays of loudspeakers, because the splaying of the sources caused the backs of more tessellae to “come into view.” More importantly, the physical requirements, as defined by Huygen’s Construction, only allowed a two-dimensional model because the wavefront most horns produce does not leave the vertical edges of the horn at the same instant that it leaves the horizontal edges. It was impossible to construct a 3D mosaic that satisfied the tessellation conditions. The models also showed less-than-measured directionality at low frequencies, and were limited to symmetrical horns.

0.2 An Improved Method: Flat Tessellation

In the current paper, we present a refinement of the tessellation technique that largely eliminates the problems mentioned. Instead of placing the tessellae in an arc along the presumed wavefront, we will arrange them in a flat plane at the mouth of the horn. However, flat tessellation, as shown in Fig. 1, violates Huygen’s principle – the condition that all the sources must lie within a common wavefront.

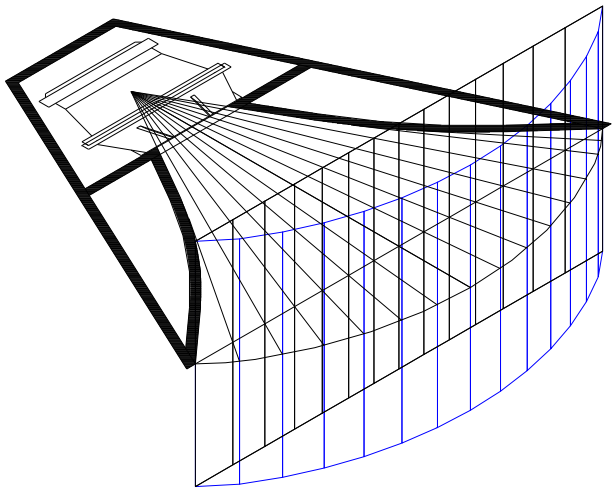

Fig. 1. Wavefront Tessellation vs. Flat Tessellation

In order to be released from Huygen's Principle, the tessellae must be represented by a more complete acoustical model. The formula used to model the off-axis response of a rectangular tessella [4] is the analytical solution of Rayleigh's Integral [2] for a rectangular aperture. Rayleigh's integral is a simplified form of the Kirchoff-Helmholtz integral, which will be discussed at some length below. By employing the complete Kirchoff-Helmholtz integral, we can model a wavefront passing at an oblique angle through the tessellae, more accurately model the low-frequency off-axis response, and accurately model the response over a much broader angle.

1 THE KIRCHHOFF-HELMHOLTZ EQUATION

1.1 Analytic Form of Equation

The Kirchhoff-Helmholtz equation is a member of the family of equations known as Boundary Integral Equations (B.I.E.'s). The formula is the mathematical realization of Kirchoff's theorem, which states: "If either the pressure or the normal particle velocity is known over an arbitrary surface surrounding a source, the acoustical field due to that source can be calculated at any given point in space [2][5][6]."

In "Loudspeaker Acoustical Field Calculation with Application to Directional Response Measurement," by Gunness and Mihelich [6], the Kirchhoff-Helmholtz equation is derived in various forms appropriate to different applications. The complete frequency-domain equation is:

$$p(\vec{x}) = \frac{\rho}{4\pi}\iint \frac{-j\omega\hat{v}_n(x_S)e^{jkR}}{R}dS + \frac{1}{4\pi}\iint (e_R \cdot n_S)\left(-jk + \frac{1}{R}\right)\frac{\hat{p}(x_S)}{R}e^{jkR}dS \quad (1)$$

where:
S is an arbitrary surface completely enclosing all sources of sound.
x_s is any point on the surface, S.
$\vec{x}$ is any point outside the surface.
e_R is the unit vector from x_s to x.
R is the distance from x_s to $\vec{x}$.
n_S is the unit vector normal to the surface at x_s.
$\hat{v}_n(x_S)$ is the normal velocity at various points, x_s , on the surface.
$\hat{p}(x_S)$ is the pressure at various points, x_s, on the surface, and

$$k = \frac{\omega}{c} = \frac{2\pi f}{c}$$

These terms are depicted in Fig. 2.

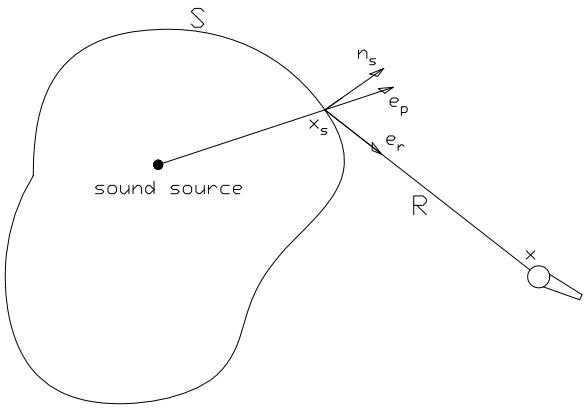

Fig. 2. Definition of Kirchhoff-Helmholtz Equation Terms

Kirchhoff's Theorem states that by integrating the pressure and velocity over the entire surface, the pressure anywhere outside the surface can be determined. Of course, in order to make practical use of this expression, we will need to represent the surface as a finite number of tessellae.

The most general form of this equation contains two main parts: a term containing the velocity, and a term containing the pressure. However, velocity and pressure cannot be specified independently. Given one parameter, there is only one valid value for the

other parameter. It will be most convenient if we restate velocity in terms of pressure. As given in [6],

$$\hat{v}_n(x) = \frac{1}{\rho c}(\cos\ \theta \hat{p}(x) - \frac{1}{jk}(n_s \cdot \nabla \hat{p}(x)) \quad (2)$$

$\nabla\hat{p}(x)$ is the pressure gradient. The dot product with the normal vector gives the normal component of the gradient – a scalar. Likewise in the first term, cosθ gives the normal component. Notice that the velocity has a real term and an imaginary term. The real part is independent of the shape of the field – giving the same result for a plane wave as it does for a spherical wave. The imaginary term goes to zero in a plane wave, and is very large near the origin of a spherical wave.

Substituting (2) into (1) yields:

$$p(x) = \frac{1}{4\pi}\iint\left[\frac{jk\hat{p}(x_S)\cos\theta}{R} + \frac{jk\hat{p}(x_S)(e_R \cdot n_S)}{R} + \frac{\hat{p}(x_S)(e_R \cdot n_S)}{R^2} + \frac{\cos\theta|\nabla\hat{p}(x)|}{R}\right]e^{jkR}dS \quad (3)$$

Bringing "jk" out of the integral will clarify the roles of the various terms.

$$p(x) = \frac{jk}{4\pi}\iint\left[\frac{\hat{p}(x_S)\cos\theta}{R} + \frac{\hat{p}(x_S)(e_R \cdot n_S)}{R} + \frac{\hat{p}(x_S)(e_R \cdot n_S)}{jkR^2} + \frac{\cos\theta|\nabla\hat{p}(x)|}{jkR}\right]e^{jkR}dS \quad (4)$$

This equation has four terms that can be analyzed separately.

$$p(x) = \frac{jk}{4\pi}\iint[Term1 + Term2 + Term3 + Term4]e^{jkR}dS \quad (5)$$

Term1, $\frac{\hat{p}(x_S)\cos\theta}{R}$, is the high frequency, monopole (omnidirectional) term resulting from the real part of the normal velocity. This is the term that constitutes the Rayleigh integral. For far-field analysis of a rectangular tessella with propagation normal to the surface, the entire term can be moved outside the integral. The remaining double integral contains only e^{jkR}. If we set the limits of the double integral to the dimensions of the rectangular source, we have a definite integral which is easily solved - giving the expression reported in Olson (a product of two sinc functions) [4].

Term 2, $\frac{\hat{p}(x_S)(e_R \cdot n_S)}{R}$, is a high frequency, dipole term resulting from the pressure distribution over the surface. The dot product, $e_r \cdot n_s$, can be expressed as cosφ, where φ is the off-axis angle of the observation point. Its value is 1 at 0° (on axis), zero at 90°, and –1 at 180°. This directional behavior is described as a figure-eight polar pattern.

Term 3, $\frac{\hat{p}(x_S)(e_R \cdot n_S)}{jkR^2}$, is a low frequency, near field, dipole term resulting from the pressure distribution over the surface. For high frequencies, 1/k approaches zero. For large distances, $1/R^2$, becomes small in comparison to 1/R. For horn mouth modeling, this term is typically negligibly small. However, its similarity to term 2 makes it very inexpensive to calculate (Term2/jkR), so there is no reason not to incorporate it in numerical methods.

Term 4, $\frac{\cos\theta|\nabla\hat{p}(x)|}{jkR}$, is a low frequency, monopole term resulting from the imaginary part of the normal velocity. It is often referred to as the divergence term because it is only non-zero in a divergent field, such as that near a point source. A complete treatment of this term requires consideration of the diffraction around the perimeter of a horn. It has a negigible effect on directionality, because it has the same form as Term 1, which is already larger than Term 2 at low frequencies. It does, however, have an effect on the absolute pressure response at low frequencies, so it cannot be ignored if pressure measurements at the mouth are to be used to predict far-field low frequency response. In the technique being explored here, we will be forcing the on-axis response to match an axial measurement, so the term can be ignored without much effect. See [6] for a more thorough discussion.

Let us consider the effect of the additional terms, intuitively. One difference between the new and the old tessella is that an individual new tessella will contribute very little in the reverse direction. If θ is zero (normal propagation), terms 1 & 2 exactly cancel at 180° off axis. Note that the output of the overall model doesn't go to zero – just the contribution of that one tessella. Another effect is that the contribution of term1 typically varies across the mouth of a horn (the inclination angle is zero at the center and non-zero at the edge), while the contribution of term 2 varies with observation angle.

1.2 Numerical Implementation of the K-H Integral

In order to apply the K-H integral to a numerical method, it will have to be converted to a summation. The technique of tessellation can be expressed as:

$$p(x) = \sum_n \left(\frac{jk}{4\pi R} \left[\cos\theta_p + (e_R \cdot n_S) + \frac{j(e_R \cdot n_S)}{kR} \right] \int_{z_1}^{z_2} \int_{y_1}^{y_2} \hat{p}(x_S) e^{jkR} dy dz \right) \quad (6),$$

This is a summation of the n tessellae that comprise the surface. The expression within the parentheses represents the analytic solution for an individual tessella. The expression within the square brackets represents the part of terms 1, 2 & 3 that are taken as constant over the surface of the tessella (term 4 is ignored, for the reasons discussed previously). The double integral is presented in the form for a rectangular tessella that is y_2-y_1 wide, and z_2-z_1 high. It can be converted to represent a tessella of any shape, by selecting suitable variables and limits [reference – possibly Rayleigh]. For instance, a round tessella can be represented by replacing "dy dz" by "r dr dθ", and setting the limits to [0, r] and [0, 2π]. The pressure distribution function, $\hat{p}(x_s)$, is left inside the integral,

because its phase will vary over the surface of the tessella if the propagaion direction is not perpendicular to the surface.

The original tessella, as defined in Part 1, was defined by its length, width, rotation, elevation, and azimuth. In order to implement the more complete K-H integral, we will need to specify the direction of propagation, e_p. The angle between e_p and n_s, the unit normal to the surface, is the inclination angle, θ. Besides the cosθ term in Eq. (6), the inclination angle also affects $\hat{p}(x_s)$, in the double integral. A new expression for $\hat{p}(x_s)$ is:

$$\hat{p}(x_s) = \hat{p}_0 e^{jk(y\vec{\theta}\cdot\vec{y}+z\vec{\theta}\cdot\vec{z})} \qquad (7),$$

in which $\vec{\theta}$ is the vector representation of the propagation direction relative to the tessella, with $\vec{x}$ representing the axis of the tessella direction, $\vec{y}$ representing the unit horizontal direction of the tessella (along its width), and $\vec{z}$ representing the unit vertical direction of the tessella (along its height).

When this expression is applied, the evaluation of the double integral takes the same form as for a simple tessella: the product of two sinc functions; but the argument to the sinc functions is modified. The horizontal and vertical off-axis angles are simply reduced by the horizontal and vertical propagation angles. This satisfies the obvious requirement that the narrowest impulse must occur when the propagation direction is directly toward the microphone.

2 EXAMPLE OF FLAT TESSELLATION

2.1 Example Horn

In [1], a single mid-frequency horn was measured and its directionality was compared to a tessellated model. Agreement between the modeled and measured response was roughly within 3 dB and 22° of phase for 15, 30, and 45 degree curves. After optimization, the agreement was roughly within 0.5dB and 10° of phase. Using the more complete implementation just described, the same horn can be modeled with a complete three-dimensional planar tessellation. Both horizontal and vertical directional response may then be obtained from the same model.

2.2 Horizontal Model

A horizontal model was developed, by employing the methodology described in Part I, but with flat tessellation, the more complete K-H integral, and with the driving functions adjusted for offset delay & estimated pressure. The offset delay for each tessella corresponded to the path difference between the Huygen tessellation and the flat tessellation. The estimated pressure is based on the total area of the wavefront at the section where the tessella resides. In both cases, the intent was to set the driving function to the complex pressure response we would expect to measure at the center of each tessella. By contrast, a Huygen tessellation starts with equal pressure and arrival time.

The flat tessellation is shown in Fig. 1. Fourteen 0.4064-m-tall tessellae were used. Their widths ranged from 0.0717 m for the outer column, to 0.048545 m for the inner column. Fig. 3 compares the measured and modeled directionality responses at 15°, 30°, 45°, 60°, & 75° off axis.

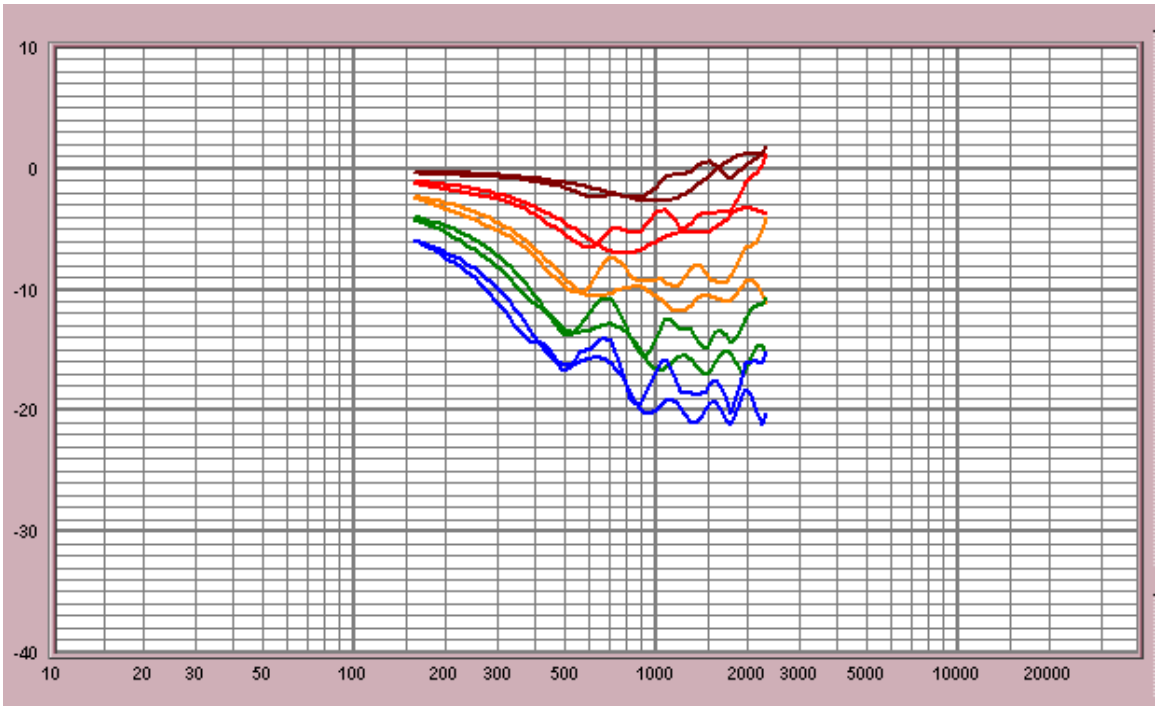

Figure 3: Modeled Vs. Measured, Unoptimized; 15°, 30°, 45°, 60°, 75° Off Axis

All five off-axis curves are comparable to the agreement of the raw model of Part 1. However, the new method achieves these results out to 90°, whereas the previous method was only accurate to 45°. Furthermore, the low frequency agreement is much better than before, even without optimization. After optimization, the results are even better (Fig. 4). Whereas the previous method produced a 6dB error at 250Hz, 90° off axis, the new method is accurate to within 0.1dB at 250 Hz.

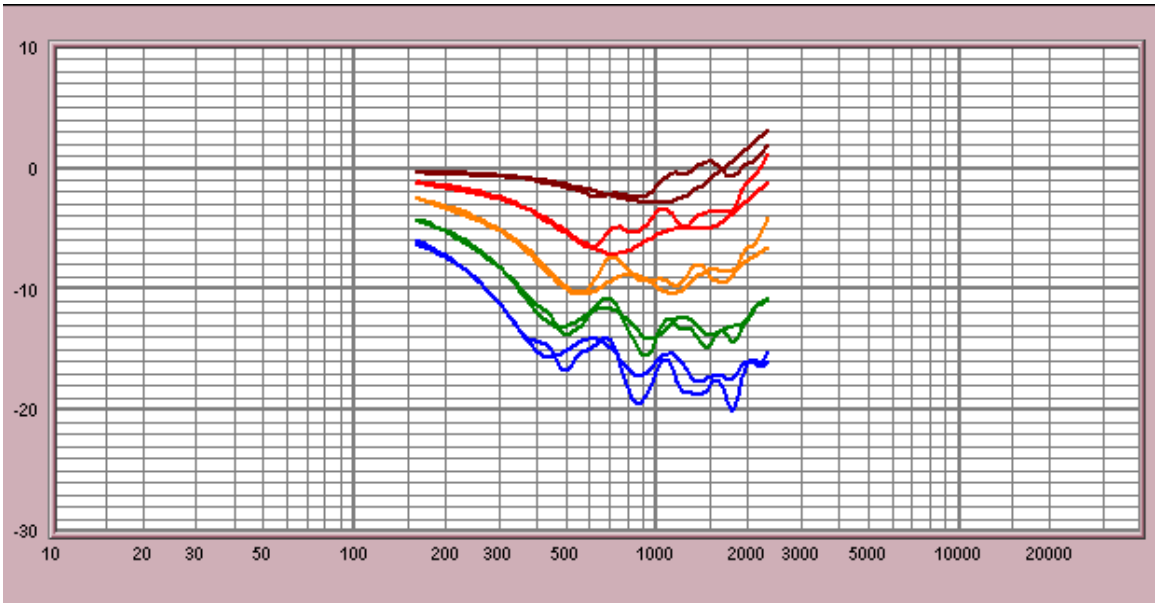

Fig. 4. Modeled Vs. Measured, Optimized; 15°, 30°, 45°, 60°, 75° Off Axis

2.3 Vertical Model

Repeating the process, a vertical model was constructed. For this case, eight 0.7112-m-wide tessellae were used. Their height ranged from 0.07105 m for the upper and lower row, to 0.060782 m for the middle row. This tessellation is shown in Fig. 5. The comparison between modeled and measured curves is shown in Fig. 6.

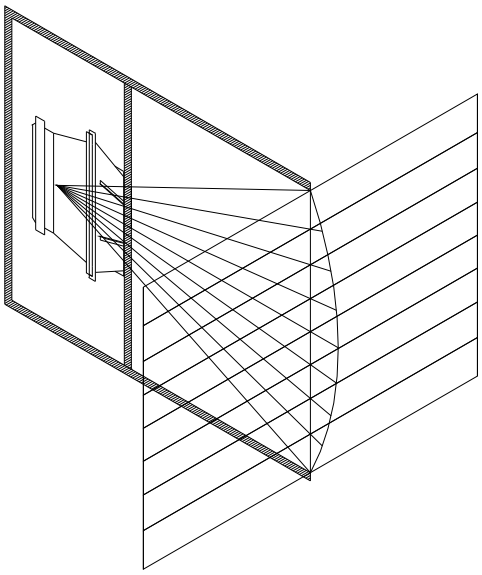

Fig. 5. Vertical Flat Tessellation

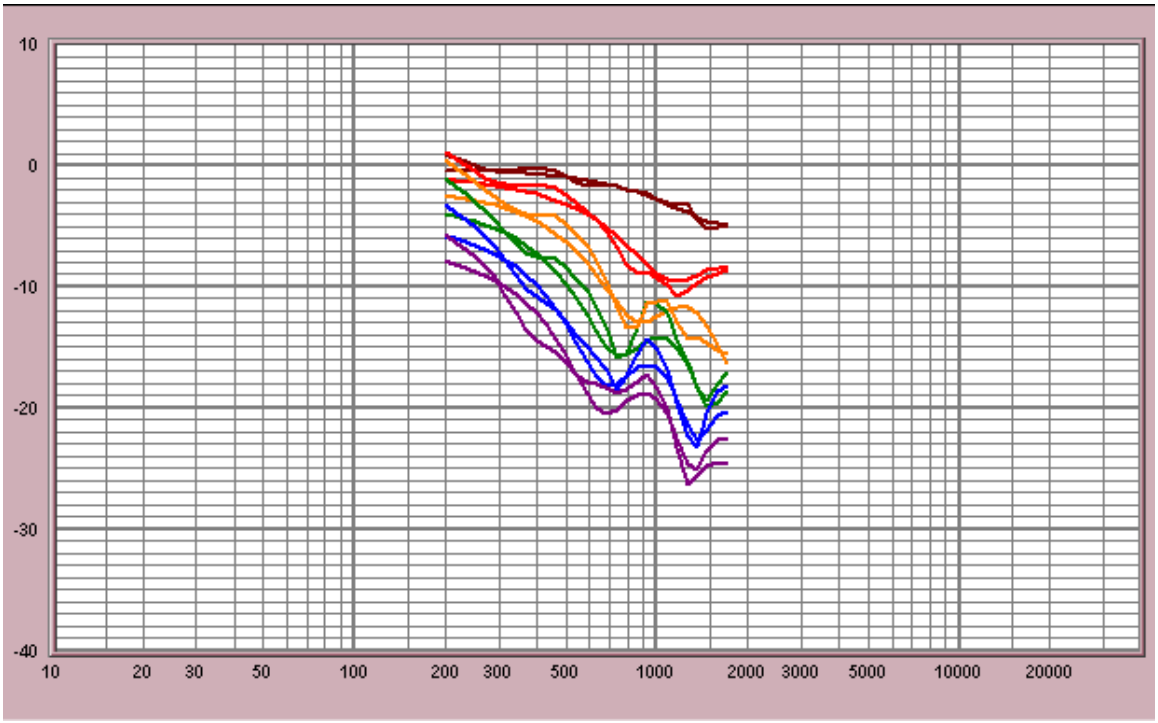

Fig. 6. Vertical Modeled Vs. Measured; 15°, 30°, 45°, 60°, 75°, and 90° Off Axis

2.4 Three-Dimensional Model

In order to build a three-dimensional model from the horizontal and vertical models, A complete tessellation is developed, as shown in Fig. 7. Then, the driving function for each tessella is initialized by using the corresponding horizontal and vertical driving functions from the optimized horizontal and vertical models. The dimensions of each tessella comprise a fraction of the total width, and a fraction of the total height. The corresponding horizontal driving function is multiplied by the tessella's vertical fraction, and the corresponding vertical driving function is multiplied by the tessella's horizontal fraction. When constructed in this way, the three-dimensional model produces the same results as the two-dimensional models in the horizontal and vertical planes.

For rectangular horn mouths, the results away from the horizontal and vertical planes (i.e., on the diagonals) will still show excellent agreement. Even so, the accuracy of the model can be further improved by applying the optimization process to the complete, 14 x 8 model. The agreement of the unoptimized three-dimensional model is shown in Fig. 8.

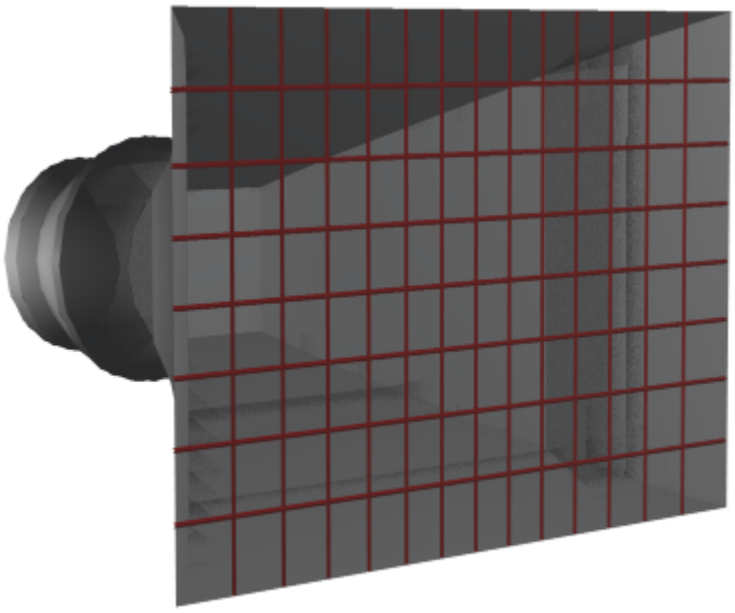

Fig. 7. Three-Dimensional Flat Tessellation

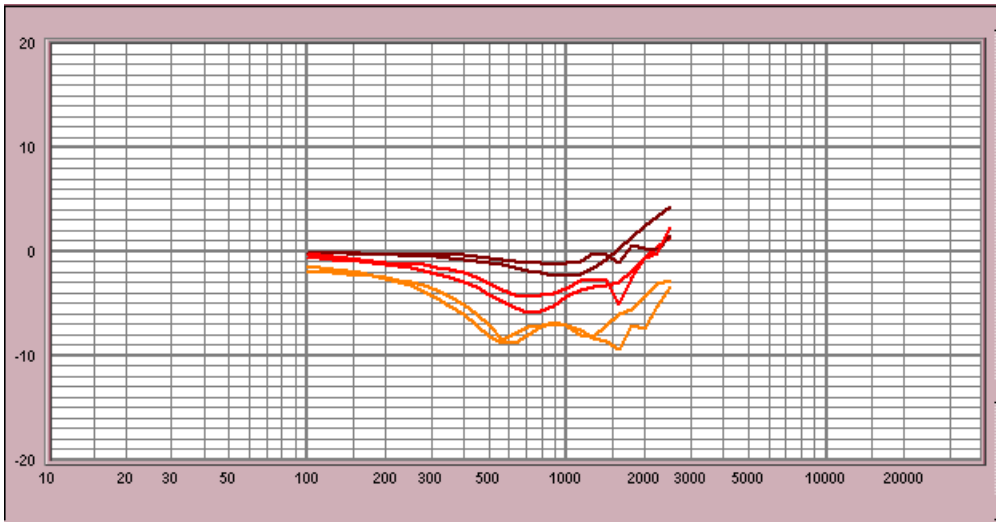

Fig. 8. Three-Dimensional Flat Tessellation Comparison (Along a Diagonal)

3 APPLICATIONS OF FLAT TESSELLATION

3.1 Automated Directional Response Measurement, by Mouth Mapping

The process described in Section 2 is primarily a synthesis process. A model synthesized from the geometry of a horn is able to predict with surprising accuracy the

detailed directional behavior of the horn. The value of this process in development work should be obvious. A horn can be evaluated with a simple software model before a prototype has been constructed. With a prototype in hand, measured data may be used to refine the model – yielding data with sufficient precision for array predictions.

Let us consider a further refinement of the technique; one which is useful for characterizing the directional behavior of an existing horn. Rather than relying on an optimizer to adjust the driving functions of the tessellae, the pressure at the center of each tessella can be measured, using the real horn. The optimizer may then be applied to the remaining estimated values (primarily propagation angle). Alternatively, a closely-spaced set of data points can be measured in order to determine the propagation direction by measurement.

The technique of measuring the pressure over the surface of the mouth is called, "mouth mapping." It is particularly useful in the case of less well-behaved horns – particularly those in which the high frequency beam is narrower than the included angle of the walls. It also offers the potential of being realized as an automated process, since the detailed CAD work can be skipped. The complex hemispherical polar response can be obtained with very high precision, requiring far fewer measurements than would be required in the far field. The data obtained also lends itself to highly efficient numerical techniques such as the Fourier Acoustics approaches presented in [7].

3.2 An Array-Prediction Application - A "Steerable" Vertical Array of Horns

A large-scale loudspeaker system has been developed, which employs a large number of individual horns and drivers [8]. The directionality of the vertical horn arrays was intended from the outset to be electronically controllable, by changing the digital signal processing applied to each element of the array. Determining the processing required to obtain the required directional consistency and musicality, however, necessitated a very involved process – a task that could not easily be transferred to the end user.

The modeling process described here has been applied to the task of predicting the response of these large arrays, with good success. While the earlier methodology was very effective in predicting the off-axis response, relative to the on-axis response [ref], considerable field work was required to obtain the desired absolute response from the system. The new technique offers much better absolute predictions. In addition, the new technique correctly accounts for the varying distance from various parts of the array to nearby listeners. Fig. 9 and Fig. 10 illustrate a portion of the array and show a typical family of response predictions, post-optimization.

A complete set of models has been constructed for the various subsystems in the illustrated array. Work is currently underway to incorporate these models into a programmed interface, which will allow the user to optimize the digital signal processor settings and provide directional predictions for use in acoustical modeling programs, such as EASE.

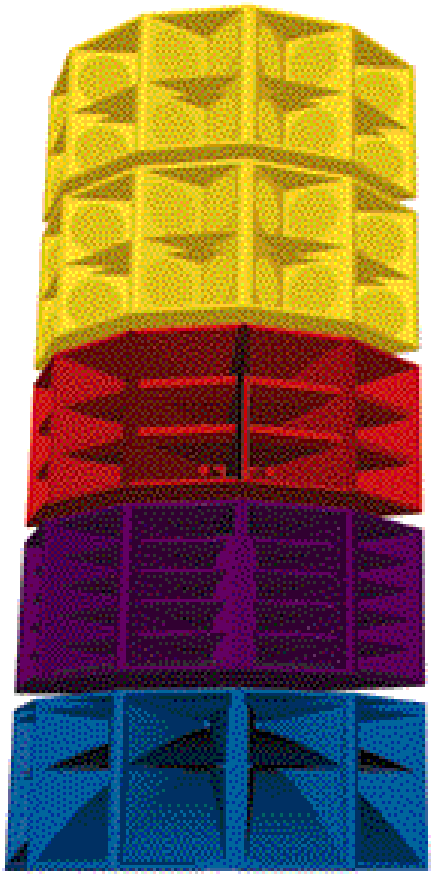

Fig. 9. Large-scale Loudspeaker System Employing Many Horns

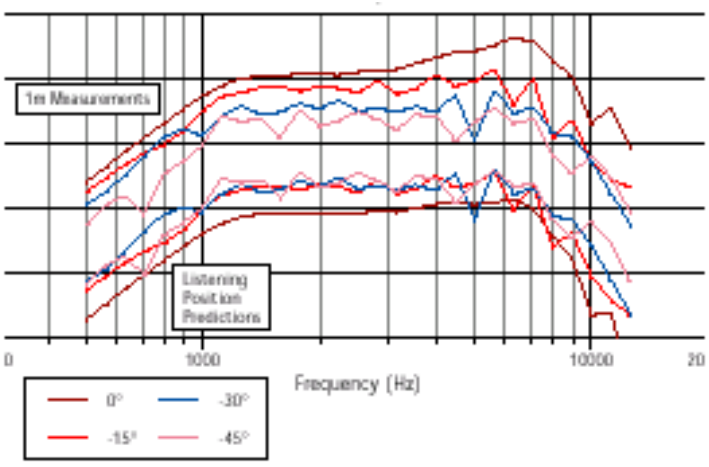

Fig. 10. Example PPST Family of Curves

4 CONCLUSIONS

4.1 Benefits of New Technique

In Part 1 of this paper, a modeling technique called tessellation was introduced. Unlike the conventional data-table approach, it offered complete immunity from various geometric error mechanisms such as apparent-apex error, produced highly accurate interpolations, and allowed accurate prediction of array interactions.

In the current installment, an improved modeling technique was presented, which allows a horn mouth to be modeled by a flat tessellation. By incorporating all four terms of the Kirchhoff-Helmholtz integral, a diverging wavefront may be accurately modeled with a planar array of source elements. The new technique is more accurate at low frequencies. It retains its accuracy to 90° off axis. And, it can be used to create a single three-dimensional model, rather than separate horizontal and vertical two-dimensional models.

The previous technique relied on Huygen's principle, and consequently, could not be applied to asymmetrical horns. Because the new technique handles non-normal propagation, it is not necessary for the wavefront to leave both edges of the horn mouth simultaneously. Therefore, asymmetrical horns can also be modeled with no loss of precision.

4.2 Future Improvements - Back Hemisphere Modeling

The full K-H tessella differs from the simple tessella employed in Part 1 in that its pressure contribution is valid even at 180° off axis from the tessella. However, the overall horn mouth model is not valid in the back hemisphere, because the paths from the tessellae to observation points in the back hemisphere are obstructed by the walls of the horn. Any sound pressure in the back hemisphere must diffract around the edges of the horn.

The edge diffraction, then, supplies the broad-band frequency response in the back hemisphere. What is probably less obvious is that edge diffraction also affects the low-frequency response in the front hemisphere. The velocity portion of the K-H integral was estimated, based on the geometry of the horn. But, as we mentioned in Section 1.1, we have ignored term 4 - the gradient term. We have used the horn geometry to estimate the wavefront expansion. But near the edge, the horn geometry underestimates the wavefront expansion. The amount of this underestimation is easily calculated, but is somewhat tricky to define in the model specifications. The question must be answered, "Which edges of which tessellae are mouth edges?"

We have identified a technique, which we will call "picture-framing", for defining the edge conditions of a horn mouth or baffle edge. With this technique an object is defined which is best described as a picture frame. When the response is desired at a location that isn't "visible" from the mouth of a horn, the picture frame object will calculate a diffracted signal, derived from the tessellated model. Low-frequency

divergence will also be calculated from the picture frame specification - so the absolute response predicted in the front hemisphere will be correct.

When two or more horns are arrayed, another larger picture frame will be created which contains the smaller picture frames which contain the tessellated mouth models. In this way, the back hemisphere radiation should be fairly accurate - even for large arrays.

REFERENCES

[1] D. W. Gunness and W. R. Hoy, “Improved Loudspeaker Array Modeling, “ presented at the 107th Convention of the Audio Engineering Society, 1999, Preprint #5020.

[2] A. D. Pierce, *Acoustics* (Mc-Graw Hill, 1981) p. 175.

[3] Lord Rayleigh, *Theory of Sound, Vol. II* (MacMillan & Co., London, 1896)

[4] H. F. Olson, *Elements of Acoustical Engineering* (Van Nostrand, New York, 1947)

[5] Jackson, John D., *Classical Electrodynamics* (John Wiley & Sons, Inc., 1975)

[6] D. W. Gunness and R. Mihelich, “Loudspeaker Acoustical Field Calculation with Application to Directional Response Measurement, “ to be presented at the 109th Convention of the Audio Engineering Society, 2000

[7] Williams, Earl G., *Fourier Acoustics, Sound Radiation and Nearfield Acoustical Holography* (Academic Press, 1999)

[8] D.W. Gunness and J. F. S. Speck, “Phased Point Source Technology and the Resultant KF900 Serires, “ (Eastern Acoustic Work, Inc., 1997).